Ab Initio MRD-CI Study of the Electronic Spectrum of $BrNO_2$ and Photofragmentation

Antonija Lesar,*,† Saša Kovačič,† Milan Hodošček,†,‡ Max Mühlhäuser,§ and Sigrid D. Peyerimhoff⊥

Department of Physical and Organic Chemistry, Institute Jožef Stefan, Jamova 39, SI-1000 Ljubljana, Slovenia, Centre for Molecular Modeling, National Institute of Chemistry, Hajdrihova 19, SI-1000 Ljubljana, Slovenia, Department of Process Engineering and Environmental Technology, Management Center Innsbruck, Egger-Lienz Strasse 120, A-6020 Innsbruck, Austria, and Institut für Physikalische und Theoretische Chemie der Universität Bonn, Wegelerstrasse 12, 53115 Bonn, Germany

Received: July 30, 2004

Multireference configuration interaction, MRD-CI, methods with the cc-pVDZ+sp and cc-pVTZ+sp basis sets were employed to determine the low-lying singlet and triplet electronic states of nitryl bromide, $BrNO_2$. The calculations predict two very strong transitions, $3^1A_1 \leftarrow X^1A_1$ and $3^1B_2 \leftarrow X^1A_1$, at 6.15 and 7.27 eV, respectively. At wavelengths that are atmospherically relevant to the $BrNO_2$ photolysis, 1^1B_2 and 1^1B_1 singlet states with vertical transition energies of 3.43 and 3.85 eV, respectively, are computed. The corresponding triplet states are lower in energy by 0.27 and 0.36 eV, respectively. Both singlet and triplet states are found to be highly repulsive along the Br−N coordinate and they dissociate to the ground-state fragments Br and NO_2. The comparison between the first singlet excited state of $BrNO_2$ and $ClNO_2$ demonstrates that the transition is red-shifted by 80 nm from $ClNO_2$ upon replacement of chlorine by bromine. Furthermore, the most intense transition $3^1A_1 \leftarrow X^1A_1$ of $BrNO_2$ has a 0.9 eV lower energy than that of $ClNO_2$. These energy differences can be explained by the large halogen character of the orbitals involved in the electron excitations.

I. Introduction

Bromine−nitrogen oxide compounds have been well established as important atmospheric species associated with processes that affect the stratospheric ozone abundance.[1,2] Under stratospheric conditions, $BrNO_2$ is possibly formed by heterogeneous reactions between HBr and N_2O_5 in polar stratospheric clouds,[3] while in the marine troposphere it is produced in the reaction of N_2O_5 with NaBr on sea-salt particles.[4] The removal of nitryl bromide and conversion to active bromine results predominantly through rapid day-time photolysis. Photolysis of $BrNO_2$ into $Br + NO_2$ contributes to the sudden ozone-depletion events occurring in the polar troposphere.[5]

The first gas-phase IR spectroscopic observation of $BrNO_2$ has been reported by Finlayson-Pitts et al.[6] There is no direct experimental determination of the structure of $BrNO_2$; however, the results of high-resolution infrared gas-phase absorption spectra[7] have indicated that the structural parameters of the NO_2 group are very similar to those of $ClNO_2$ and that the Br−N bond length is about 2.0 Å, in agreement with recent ab initio calculations.[8] Very recently, Tchana et al.[9] have determined the rotational and centrifugal distortion constants of $BrNO_2$ from investigations of the high-resolution infrared absorption spectrum of the ν_2 fundamental bands. To the best of our knowledge, work related to the UV/vis absorption cross section was only reported in the literature by Scheffler et al.[10] In the range of 185−600 nm, an intense absorption peak with a maximum at 199 nm, another considerably weaker maximum at 247 nm, and a low-intensity broad band centered at 372 nm were found.

The aim of the present study is first to provide characteristic fingerprints for identifying $BrNO_2$ in UV/vis experiments and second to understand which electronic excitations of $BrNO_2$ can lead to its photodissociation, producing active bromine in the atmosphere. We report on the study of the excited states of $BrNO_2$ with the multireference configuration interaction method and characterize the nature of the electronic transitions based on qualitative molecular orbital consideration. Details of theoretical methods used are described in the next section, while the results and discussion are presented in the following section. Conclusions are summarized in the final section.

II. Computational Methods

The equilibrium geometry of nitryl bromide ($BrNO_2$) was fully optimized by using the single and double excitation coupled-cluster method, including a perturbation estimate of the effects of connected triple excitations, CCSD(T),[11] with the 6-31G(d) basis sets, using the Gaussian 03 program package.[12]

The computations of the electronically excited states were performed with use of a CCSD(T)/6-31G(d) geometry with the multireference single and double excitation configuration interaction method, MRD-CI, implemented in the Diesel program.[13] The selection of the reference configurations by a summation threshold is carried out automatically. We used a summation threshold of 0.85, which means that the sum of the squared coefficients of all reference configurations selected for each state (root) is above 0.85. The number of reference configurations per irreducible representation (IRREP) was in the range between 8 and 17. An analysis of the molecular orbitals (MO) involved in these selected reference configurations justified the prior choice of treating the 24 valence electrons as active while the remaining electrons were kept in doubly occupied orbitals defined as frozen-core orbitals.

† Institute Jožef Stefan.
‡ National Institute of Chemistry.
§ Management Center Innsbruck.
⊥ Institut für Physikalische und Theoretische Chemie der Universität Bonn.

10.1021/jp046599x CCC: $27.50
Published on Web 10/02/2004

TABLE 1: Calculated Vertical Excitation Energies ΔE (eV) and Oscillator Strengths f to Singlet Excited States of $BrNO_2$[a]

		cc-pVDZ+sp		cc-pVTZ+sp			
state	excitation	ΔE	f	ΔE	f	ΔE_{trip}	ΔE_{exp}[b]
1^1A_1	$(5a_1)^2(4b_2)^2(1a_2)^2(2b_1)^2$	0.0	0.0	0.0	0.0		
1^1B_2	$4b_2 \rightarrow 6a_1$	3.77	0.0005	3.43	0.0001	3.16	3.33
1^1B_1	$2b_1 \rightarrow 6a_1$	4.11	0.0002	3.85	0.0007	3.49	
2^1A_2	$4b_2 \rightarrow 3b_1$	4.46	0.0	4.56	0.0	4.33	
1^1A_2	$1a_2 \rightarrow 6a_1$	5.16	0.0	4.69	0.0	4.84	
2^1B_2	$3b_2 \rightarrow 6a_1$	5.04	0.00001	4.87	0.00002	4.81	
2^1B_1	$5a_1 \rightarrow 3b_1$	4.78	0.001	4.93	0.001	5.02	
2^1A_1	$2b_1 \rightarrow 3b_1$	5.13	0.022	5.02	0.022	5.18	5.02
3^1A_2	$3b_2 \rightarrow 3b_1$	5.71	0.0	5.76	0.0	5.67	
3^1A_1	$5a_1 \rightarrow 6a_1$	6.43	0.764	6.15	0.757	3.38	6.23
3^1B_2	$1a_2 \rightarrow 3b_1$	7.76	0.242	7.27	0.293	4.31	

[a] ΔE_{trip} is relative to the ground state $^1A_1$ energy. The MO notation classifies the 24 valence electrons active in the calculations [b] From ref 10.

From this set of reference configurations (mains), all single and double excitations in the form of configuration state functions (CSFs) are generated. All configurations of this set with an energy contribution $\Delta E(T)$ above a given threshold T were selected, i.e., the contribution of a configuration larger than this value relative to the energy of the reference set is included in the final wave function. Selection thresholds of $T = 5 \times 10^{-7}$ and 10^{-8} hartrees were used for double- and triple-ζ basis sets, respectively. The effect of the configurations that contribute less than $T = 5 \times 10^{-7}$ or 10^{-8} hartrees is accounted for in the energy computation (E(MRD-CI)) by the perturbative λ-extrapolation.[14,15] The contribution of higher excitations is estimated by applying the Langhoff−Davidson correction formula

$$E(\text{MRD-CI+Q}) = E(\text{MRD-CI}) - (1 - c_0^2)[E(\text{ref}) - E(\text{MRD-CI})]/c_0^2$$

where c_0^2 is the sum of squared coefficients of the reference species in the total CI wave function and E(ref) is the energy of the reference configurations.

We computed three singlet and three triplet states per IRREP for $BrNO_2$ of C_{2v} symmetry. The number of CSFs directly included in the energy calculations is as large as 2.6 million and 3.5 million for the singlet and triplet, respectively, selected from a total space of 6.7 million and 12.5 million generated configurations, respectively. For the calculations of excited states, we used the correlation consistent AO basis sets of Dunning of double- and triple-ζ quality.[16,17] In addition both basis sets were enlarged by s-Rydberg functions located at the nitrogen and by a negative ion function for the bromine atom, thus giving the cc-pVDZ+sp and cc-pVTZ+sp basis sets. The exponents taken are $\alpha_s(N) = 0.028$ and $\alpha_p(Br) = 0.032$.

The potential energy surfaces of the ground and excited states were computed with the cc-pVDZ+sp basis set. The Br−NO_2 bond length was varied by steps in the range from 1.78 to 10 Å, while all other geometrical parameters were optimized for the ground-state curve at the CCSD(T)/6-31G(d) level of theory.

III. Results and Discussion

$BrNO_2$ has C_{2v} symmetry with 12 doubly occupied valence orbitals to form the 1^1A_1 ground electronic state. The vertical excitation energies, which are very important quantities related to the UV spectrum, were calculated with the ground-state geometry optimized at the CCSD(T)/ 6-31G(d) level, which is presented in Figure 1. Our values for bond lengths and bond angle closely coincide with those of CCSD(T)/TZ2P calculations previously reported by Lee,[8] which are stated in parentheses in the figure. In our coordinate system, the z axis is along the N−Br bond, and the oxygen atoms lie in the yz plane.

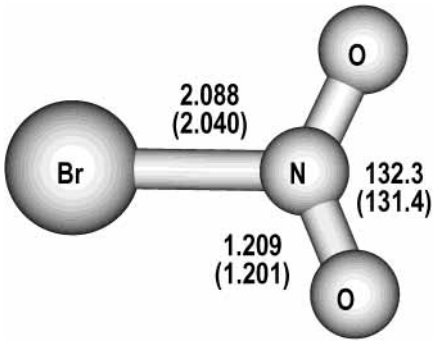

Figure 1. CCSD(T)/6-31G(d) equilibrium geometry of nitryl bromide, $BrNO_2$, with the CCSD(T)/TZ2P values [ref 8] in parentheses. The bond lengths are given in Å, bond angles in deg.

Electronic Spectrum of $BrNO_2$. Table 1 summarizes the calculated vertical excitation energies and oscillator strengths of the present investigations. We include the computed values of the cc-pVDZ+sp and cc-pVTZ+sp basis sets for the singlet states and only the latter basis set for the corresponding triplet excitations. As can be seen from the table, the calculated singlet excitation energies and corresponding oscillator strengths for both basis sets are quite close. The energies obtained with the basis set of double-ζ quality are within about 0.5 eV, with most being within 0.3 eV of those resulting from calculations with the triple-ζ basis set. Thus, we believe that our calculated excitation energies have an error on the order of 0.3 eV.

In Figure 2 we present the SCF-MO energy scheme of valence orbitals of $BrNO_2$ and in Figure 3 some important molecular orbital contour plots are shown. The ground-state configuration of $BrNO_2$ is $(5a_1)^2(4b_2)^2(1a_2)^2(2b_1)^2$ with regard to the 24 valence electrons treated as active in the CI calculations. The highest occupied molecular orbital HOMO $4b_2$ corresponds to a bromine p_y function plus some contribution from the oxygen in-plane lone pairs, while the lowest unoccupied molecular orbital LUMO $6a_1$ can be considered to be an antibonding σ^*(Br−N) type MO. The MO $3b_1$ is $\pi^*(NO_2)$ antibonding judged on the basis of a nodal plane between the N and O centers. On the other hand, MO $5a_1$ shows a σ(Br−N) bonding character mediated by a p_z function on Br and N. The MO $1a_2$ corresponds to a negative linear combination (π^* character) of n(O) type lone-pair orbitals at the oxygen centers, whereas MO $2b_1$ is dominated by the bromine p_z function.

The vertical excitation energy for the first singlet excited state, 1^1B_2, is 3.43 eV above the ground state. It originates from the valence MO $4b_2$ and populates MO $6a_1$, thus, it is an n $\rightarrow$ σ^*(N−Br) type transition or the HOMO $\rightarrow$ LUMO excitation.

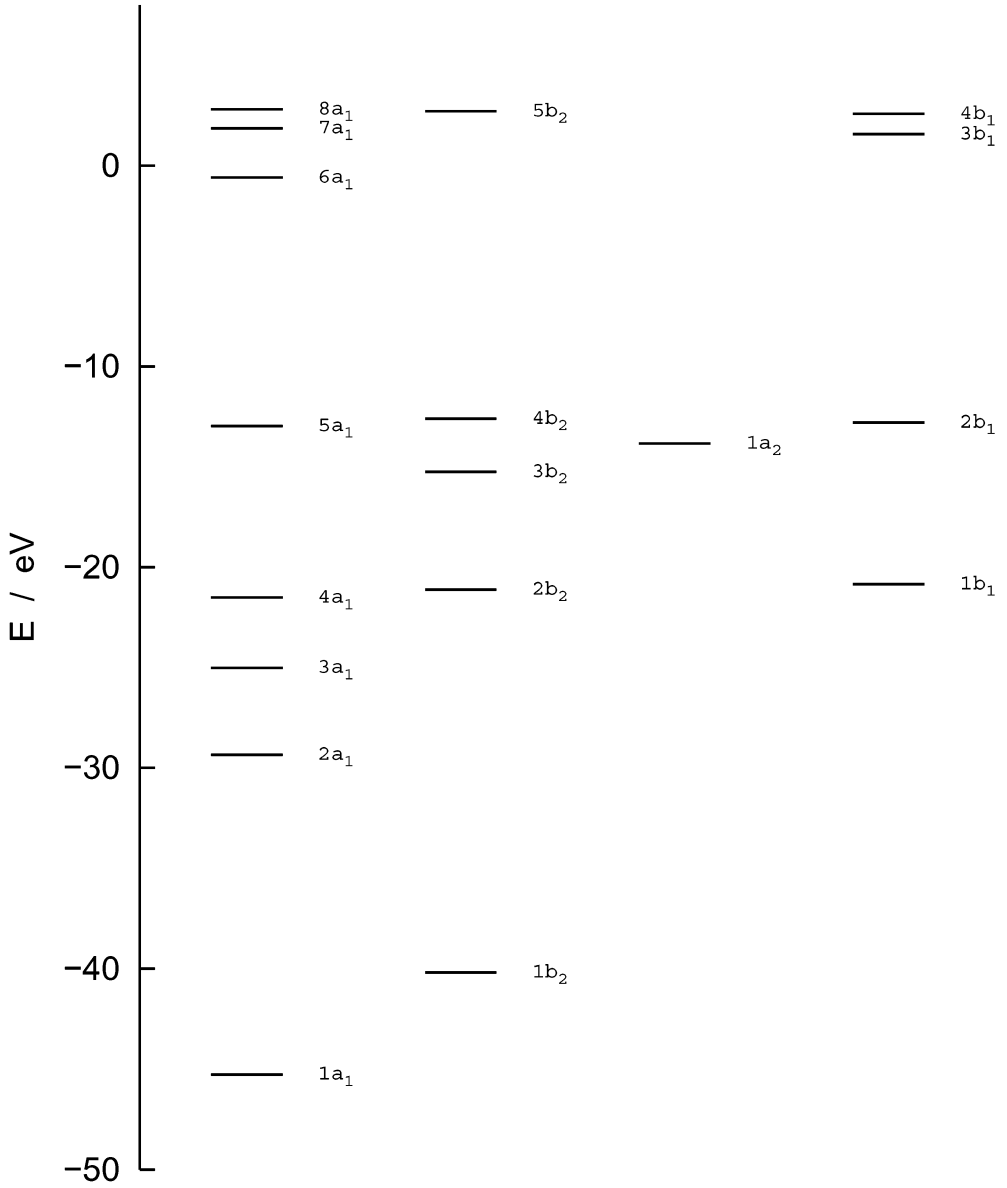

Figure 2. Schematic diagram of the molecular orbital energy spectrum of the ground-state configuration of $BrNO_2$, C_{2v} symmetry, obtained at the SCF level.

The second singlet electronic transition, $2b_1 \rightarrow 6a_1$, is predicted to occur at 3.85 eV. The oscillator strengths for these two states suggest that both transitions should be weak. In each of these lower orbitals, $4b_2$ and $2b_1$, the character of the bromine p (p_y and p_x, respectively) is very strong so that a comparable transition energy into the $6a_1$ MO and similar transition intensities are expected. The dominant transition $3^1A_1 \leftarrow X^1A_1$ of the electronic absorption spectrum is characterized at 6.15 eV as having a large oscillator strength, $f = 0.76$, and can be considered as $\sigma \rightarrow \sigma^*$(Br−N). The transition $3^1B_2 \leftarrow X^1A_1$ that corresponds to $1a_2 \rightarrow 3b_1$ is computed to be 7.27 eV. This transition can be considered as a $\pi^*(O_2) \rightarrow \pi^*(NO_2)$ type, for which a medium size oscillator strength of $f = 0.30$ could be expected. Further, a $2^1A_1 \leftarrow X^1A_1$ transition corresponds to $2b_1 \rightarrow 3b_1$ and is computed to be 5.02 eV. It shows a somewhat smaller *f*-value of 0.02, which is in line with the observation that in the low $2b_1$ MO the charge density is located largely at the bromine, leading to a n(Br) $\rightarrow \pi^*(NO_2)$ type transition, which gets its oscillator strength mainly from charge transfer.

A triplet → singlet transition is generally forbidden due to the spin conversation but the presence of the heavy bromine atom in $BrNO_2$ led to the expectation that such a transition could occur. Recent photodissociation experimental studies have revealed that for HOBr,[18] HOCl, and NOCl[19] the spin−orbit coupling is strong enough to allow a weak transition to the triplet states. Thus, we have also considered the vertical excitation energy for the lowest triplet excited state; these values are given in Table 1. The first triplet state, 1^3B_2, is lower in energy by 0.27 eV than its corresponding singlet 1^1B_2. For most states up to 5 eV, the singlet−triplet splitting is in the order of 0.1 to 0.4 eV. This is expected for transitions from in-plane to out-of-plane orbitals (from $4b_2$ or $5a_1$ to $3b_1$, or $1a_2$ and $2b_1$ to $6a_1$, for example) or if charge transfer occurs from one part of the molecule to another, so that both MOs involved have a small overlap ($2b_1 \rightarrow 3b_1$, for example). The energies of 2^3B_1 and 2^3A_1 are erroneously calculated to be slightly above the corresponding singlet energies, but the results are expected to lie within the error limits mentioned earlier (about 0.3 eV). The singlet−triplet splittings for the states resulting from $5a_1 \rightarrow 6a_1$ and $1a_2 \rightarrow 3b_1$ transitions are sizable, about 2.9 eV. This result is also consistent with empirical values for $\sigma \rightarrow \sigma^*$ and $\pi \rightarrow \pi^*$ transitions. In both cases, upper and lower orbitals have their charge densities in similar regions of the space and the large overlap leads to sizable exchange integrals, which are important

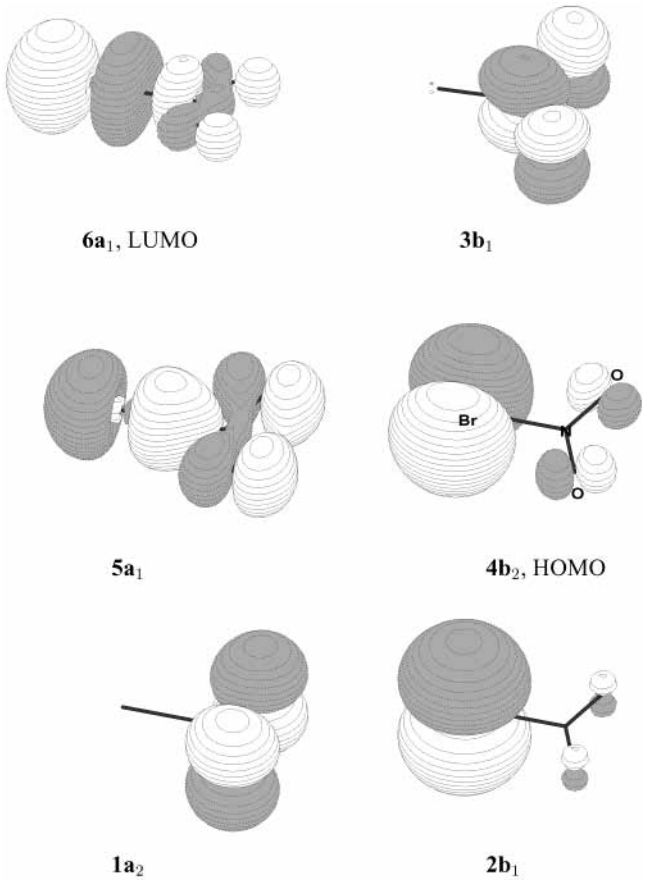

Figure 3. Charge density contours of characteristic occupied valence orbitals ($5a_1$, $4b_2$, $1a_2$, $2b_1$) and the lowest unoccupied molecular orbitals ($6a_1$, $3b_1$) of $BrNO_2$.

in the description of this energy gap. Such a large singlet−triplet splitting (3.4 eV) has also been observed for the B_2 ($1a_2 \rightarrow 2b_1$) state in ozone[20] in which the $1a_2$ and $2b_1$ orbitals are very similar to the present MOs $1a_2$ and $3b_1$.

The Potential Energy Curves for $BrNO_2$. We have also explored the potential energy surface for the C_{2v} symmetric fragmentation pathway along the Br−N bond for the lowest singlet and triplet states of the $BrNO_2$, and found the curves which are illustrated in Figures 4 and 5, respectively. The calculations were carried out at the MRD-CI/cc-pVDZ+sp level of theory. As shown in Figure 4, the ground state, 1^1A_1, is bound with a Br−N coordinate. The 1^1B_2 and 1^1B_1 states populating the σ^*(Br−N) antibonding $6a_1$ orbital and π^*(NO_2) antibonding $3b_1$ orbitals, respectively, are highly repulsive, implying that direct and fast photodissociation should occur, leading to the ground-state products, $Br(^3P) + NO_2(1^2A_1)$. The 3^1A_1 and 3^1A_2 states dissociate to NO_2 in its first excited state. The 2^1B_2 state is slightly repulsive and correlates with the dissociation channel that corresponds to the NO_2 in its second excited state. Between 4 and 5 eV, various crossings of states occur, so that excitation in this energy range can lead to various excited-state NO_2 products.

As can be expected and is evident from Figure 5, the first triplet excited state, 1^3A_1, has a repulsive character and, together with the 1^3B_2 and 1^3B_1 states, dissociates to the ground-state fragments. The 2^3A_1, 2^3B_2, and 2^3A_2 curves show shallow minima and lead to NO_2 in its first excited state.

A Comparison of the $BrNO_2$ and $ClNO_2$ Low-Lying Excited States. The UV absorption spectrum of nitryl bromide has been studied by Scheffler et al.[10] in the range of 185−600 nm. The strong absorption band found at 199 nm (6.2 eV) coincides with our computed value of 6.15 eV for the 3^1A_1 state having a large oscillator strength and the less intense peak centered at 247 nm (5.0 eV) agrees with the transition energy of 5.02 eV for the 2^1A_1 state calculated in this work. There are three candidate states which can account for the observed weak and broad band with its maximum at 372 nm (3.3 eV). Computed energies for the lowest singlet, 1^1B_2 (3.43 eV), and two triplet, 1^3B_2 (3.16 eV) and 1^3B_1 (3.49 eV), excited states all lie within this absorption energy.

The absorption spectrum of the chlorine analogue has been studied by both experiments[21,22] and ab initio calculations[23] and the theoretical results are consistent with the experimental findings. Thus, it is of interest to compare $BrNO_2$ and $ClNO_2$ excited states and photodissociations and establish the extent to which the NO_2 chromophore is independent of the halogen group. In our previous study on the low-lying excited states of $ClNO_2$,[23] the same methods and number of active electrons were used as were used for $BrNO_2$ in this work so that a realistic comparison is possible.

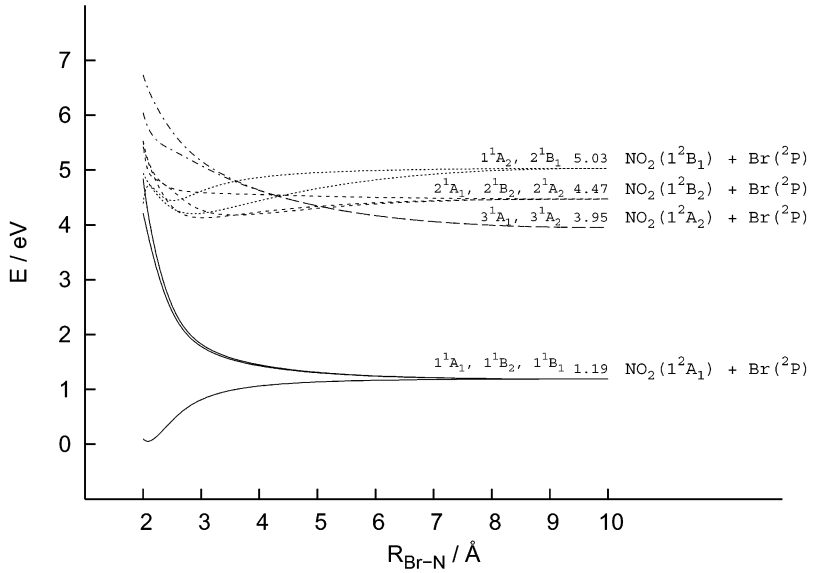

Figure 4. Calculated MRD-CI potential energy curves of the low-lying singlet states of $BrNO_2$ along a C_{2v} symmetric fragmentation pathway breaking the Br−N bond.

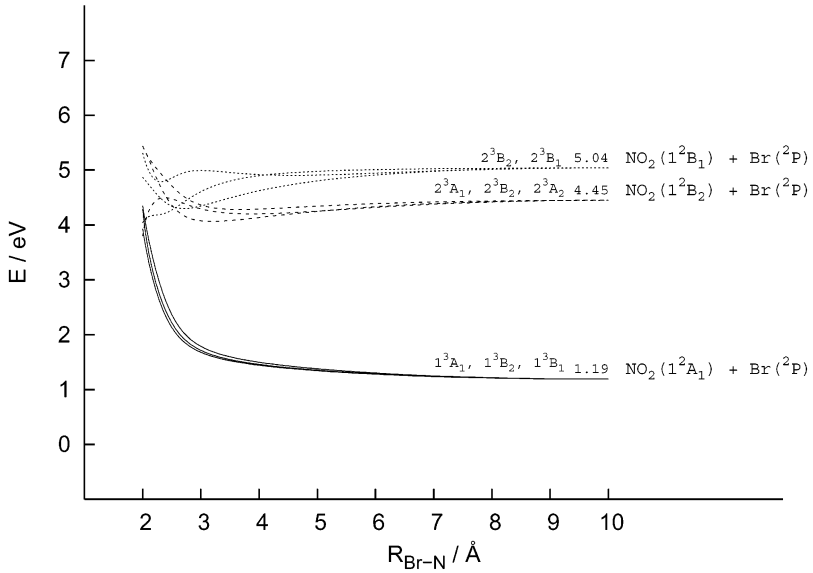

Figure 5. Calculated MRD-CI potential energy curves of the low-lying triplet states of $BrNO_2$ along a C_{2v} symmetric fragmentation pathway breaking the Br−N bond.

When the calculated electronic transitions related to the first singlet excited state of $BrNO_2$ (3.43 eV) and $ClNO_2$ (4.41 eV) are compared, it is seen that the bromine analogue lies nearly 1 eV lower, i.e., the transition is red-shifted by 80 nm from $ClNO_2$ upon replacement of chlorine by bromine. The vertical transition energy for the first intense peak (6.15 eV) is lower by 0.89 eV compared to $ClNO_2$ (7.04 eV) and thus red-shifted by 26 nm if chlorine is replaced by bromine. The principal character of the states is the same in both systems, but the more diffuse charge density in bromine leads to lower energy differences, in particular if the orbitals are involved with the dominant halogen character. The next intense transition in both molecules ($f = 0.30$) arises from the $1a_2 \rightarrow 3b_1$ excitation; these orbitals are characterized (Figure 3) as $\pi^*(O_2)$ and $\pi^*(NO_2)$ and therefore a shift does not occur ($ClNO_2$ calculated as 7.25 eV). Somewhat less intense (f around 0.02) transitions of the $2^1A_1 \leftarrow X^1A_1$ or n(X) $\rightarrow \pi^*(NO_2)$ type are located at 5.02 (247 nm) and 5.77 eV (215 nm) for $BrNO_2$ and $ClNO_2$, respectively, suggesting that they are relatively well separated and should be spectrally resolved.

Consistent with $ClNO_2$, the first triplet excited state of $BrNO_2$ is predicted to be lower than its first singlet excited state. The differences of 0.39 and 0.27 eV were found for $ClNO_2$ and $BrNO_2$, respectively.

Generally, the calculated photofragmentation along the X−N coordinate exhibits a similar behavior. Excitation of both $BrNO_2$ and $ClNO_2$ can lead to the NO_2 product in its ground and electronically excited states. For $ClNO_2$ this is consistent with experimental findings.[24,22]

Finally, there are interesting atmospheric implications of the obtained results. For $BrNO_2$ and $ClNO_2$, the absorption into the first excited state occurs at 361 and 281 nm, respectively. Significant actinic flux that is available at these wavelengths, particularly at that concerning bromine analogues, occurs at the heights between 20 and 30 km in the atmosphere, thus in the lower stratosphere, where stratospheric ozone is produced. This implies that photolysis of these molecules could be a possible source of bromine and chlorine atoms, which are known to be active in the ozone destruction cycle.

IV. Summary

Vertical excitation energies for the low-lying singlet and triplet electronic states have been calculated for the $BrNO_2$ molecule with use of ab initio MRD-CI methods with a triple-ζ correlation consistent basis set enlarged by s(N) and p(Br) long-range functions. The two lowest singlet states with calculated vertical excitation energies below 4 eV arise from $n \rightarrow \sigma^*$(N−Br) excitations and transitions to them are relatively weak. The corresponding triplet states are by 0.27 and 0.36 eV, respectively, lower in energy. The dominant transitions in the electronic spectrum of $BrNO_2$ are located at 6.15 eV ($3^1A_1 \leftarrow X^1A_1$) and 7.27 eV ($3^1B_2 \leftarrow X^1A_1$) and are considered as $\sigma \rightarrow \sigma^*$(Br−N) and $\pi^*(O_2) \rightarrow \pi^*(NO_2)$ types, respectively. Further, the transition calculated at 5.02 eV ($2^1A_1 \leftarrow X^1A_1$, n(Br) $\rightarrow \pi^*(NO_2)$ type) is found to have moderate intensity. The calculated excitation energies of the 3^1A_1 state (6.15 eV) and the 2^1A_1 state (5.02 eV) are in good agreement with the strong absorption peak at 199 nm (6.2 eV) and the less intense peak at 247 nm (5.0 eV) observed in the experimental spectrum of $BrNO_2$ by Scheffler et al.[10] A low-intensity broad band centered at 372 nm (3.3 eV) most probably involves the lowest singlet, 1^1B_2 (3.43 eV), and two triplet, 1^3B_2 (3.16 eV) and 1^3B_1 (3.49 eV), excited states.

1^1B_2, 1^1B_1, 1^3B_2, and 1^3B_1 states of $BrNO_2$ are highly repulsive along the Br−N coordinate and dissociate to the ground-state fragments. This implies that absorption into these states should lead to direct and fast photolysis of $BrNO_2$ in the lower stratosphere.

When the electronic transitions related to the first excited singlet state of $BrNO_2$ (3.43 eV) and $ClNO_2$ (4.41 eV) are compared, it is seen that the transition in the bromine analogue lies nearly 1 eV lower than that in the chlorine compound. The $3^1A_1 \leftarrow X^1A_1$ transition of $BrNO_2$ has a 0.9 eV lower energy that that of $ClNO_2$, while the energy of the $3^1B_2 \leftarrow X^1A_1$ transition is the same for both species. In general, the excitations related to the transitions involving orbitals with a halogen character are from 0.6 to 1.2 eV lower in energy in $BrNO_2$ than in the corresponding excitations for $ClNO_2$.

Acknowledgment. This work was funded by the Ministry of Education, Science and Sport of Slovenia (grant number P2-0148 and partly by grant number SI-AT/04-04/20). The authors thank M. Hanrath for assistance in DIESEL program.

Note Added in Revision: We are grateful to an anonymous referee for bringing to our knowledge a contribution at the *Dijon*

2003 Conference by F. K. Tchana et al., where the following experimental structure of $BrNO_2$ was presented: $r(Br-N) = 2.0118$ Å, $r(N-O) = 1.1956$ Å, and $\angle(O-N-O) = 131.02°$. This is in good agreement with CCSD(T)/6-31G(d) and CCSD(T)/TZ2P results (Figure 1).

References and Notes

(1) Wofsy, S. C.; McElory, M. B.; Young, Y. L. *Geophys. Res. Lett.* **1975**, *2*, 215.

(2) Wennberg P. O.; Cohen, R. C.; Stimpfle, R. M.; Koplow, J. P.; Anderson, J. G.; Salawitch, R. J.; Fahey, D. W.; Woodbridge, E. L.; Keim, E. R.; Gao, R. S.; Webster, C. R.; May, R. D.; Toohey, D. W.; Avallone, L. M.; Proffitt, M. H.; Loewenstein, M.; Podolske, J. R.; Chen, K. R.; Wofsy, S. C. *Science* **1994**, *266*, 398.

(3) Hanson, D. R.; Ravishankara, A. R. *J. Phys. Chem.* **1992**, *96*, 9441.

(4) Finlayson-Pitts, B. J.; Livingston, F. E.; Berko, H. N. *Nature* **1990**, *343*, 622.

(5) Barrie, L. A.; Bottenheim, J. W.; Hart, W. R. *J. Geophys. Res.* **1994**, *99*, 25313.

(6) Finlayson-Pitts, B. J.; Livingston, F. E.; Berko, H. N. *J. Phys. Chem.* **1989**, *93*, 4397.

(7) Orphal, J.; Frenzel, A.; Grothe, H.; Redlich, B.; Scheffler, D.; Willner, H.; Zetzsch, C. *J. Mol. Spectrosc.* **1998**, *191*, 88.

(8) Lee, T. J. *J. Phys. Chem.* **1996**, *100*, 19847.

(9) Tchana, F. K.; Orphal, J.; Kleiner, I.; Redlich, B.; Scheffler, D.; Mbiake, R.; Bouba, O. *J. Mol. Spectrosc.* **2002**, *216*, 292.

(10) Scheffler, D.; Grothe, H.; Willner, H.; Frenzel, A.; Zetzsch, C. *Inorg. Chem.* **1997**, *36*, 335.

(11) Pople, J. A.; Gordon, M. H.; Raghavachari, K. *J. Chem. Phys.* **1987**, *87*, 5968.

(12) Frisch, M. J.; Trucks, G. W.; Schlegel, H. B.; Scuseria, G. E.; Robb, M. A.; Cheeseman, J. R.; Montgomery, J. A.; Vreven, T., Jr.; Kudin, K. N.; Burant, J. C.; Millam, J. M.; Iyengar, S. S.; Tomasi, J.; Barone, V.; Mennucci, B.; Cossi, M.; Scalmani, G.; Rega, N.; Petersson, G. A.; Nakatsuji, H.; Hada, M.; Ehara, M.; Toyota, K.; Fukuda, R.; Hasegawa, J.; Ishida, M.; Nakajima, T.; Honda, Y.; Kitao, O.; Nakai, H.; Klene, M.; Li, X.; Knox, J. E.; Hratchian, H. P.; Cross, J. B.; Adamo, C.; Jaramillo, J.; Gomperts, R.; Stratmann, R. E.; Yazyev, O.; Austin, A. J.; Cammi, R.; Pomelli, C.; Ochterski, J. W.; Ayala, P. Y.; Morokuma, K.; Voth, G. A.; Salvador, P.; Dannenberg, J. J.; Zakrzewski, V. G.; Dapprich, S.; Daniels, A. D.; Strain, M. C.; Farkas, O.; Malick, D. K.; Rabuck, A. D.; Raghavachari, K.; Foresman, J. B.; Ortiz, J. V.; Cui, Q.; Baboul, A. G.; Clifford, S.; Cioslowski, J.; Stefanov, B. B.; Liu, G.; Liashenko, A.; Piskorz, P.; Komaromi, I.; Martin, R. L.; Fox, D. J.; Keith, T.; Al-Laham, M. A.; Peng, C. Y.; Nanayakkara, A.; Challacombe, M.; Gill, P. M. W.; Johnson, B.; Chen, W.; Wong, M. W.; Gonzalez, C.; Pople, J. A. *Gaussian 03*, Revision B.03; Gaussian, Inc.: Pittsburgh, PA, 2003.

(13) Hanrath, M.; Engels, B. *Chem. Phys.* **1997**, *225*, 197.

(14) Buenker, R. J.; Peyerimhoff, S. D. *Theor. Chim. Acta* **1974**, *35*, 33.

(15) Buenker, R. J.; Peyerimhoff, S. D. *Theor. Chim. Acta* **1975**, *39*, 217.

(16) Dunning, T. H., Jr. *J. Chem. Phys.* **1989**, *90*, 1007.

(17) Woon, D. E.; Dunning, T. H., Jr. *J. Chem. Phys.* **1993**, *98*, 1358.

(18) Barnes, R. J.; Lock, M.; Coleman, J.; Sinha, A. *J. Phys. Chem.* **1996**, *100*, 453.

(19) Bay, Y. Y.; Qian, C. X. W.; Iwata, I.; Segal, G. A.; Reisler, H. *J. Chem. Phys.* **1989**, *90*, 3903.

(20) Banichevich, A.; Peyerimhoff, S. D. *Chem. Phys.* **1993**, *174*, 93.

(21) Illies, A. J.; Takacs, G. A. *J. Photochem.* **1976**, *6*, 35.

(22) Furlan, A.; Haeberli, M. A.; Huber, J. R. *J. Phys. Chem. A* **2000**, *104*, 10392.

(23) Lesar, A.; Hodošček, M.; Mühlhäuser, M.; Peyerimhoff, S. D. *Chem. Phys. Lett.* **2004**, *383*, 84.

(24) Carter, R. T.; Hallou, A.; Huber, J. R. *Chem. Phys. Lett.* **1999**, 310, 166.